

La Thuile 2002

SUSY PRECISION MEASUREMENTS AT THE LINEAR COLLIDER

SLEPTON MASS MEASUREMENTS:

SELECTRONS, SMUONS

NEUTRALINO MASSES AND PHASES

FLAVOR VIOLATION

Acknowledgments to

Claus Bloechinger

David Miller

Michael Peskin

Jonathan Feng, H.S. Chen

The greatest challenge for our understanding of supersymmetry will be our capability to determine a key set of its ~120 parameters:

masses

couplings

phases

mixing parameters ...

Let us start with

SLEPTON MASSES

$\tilde{e}_R, \tilde{e}_L \quad \tilde{\mu}_R, \tilde{\mu}_L$

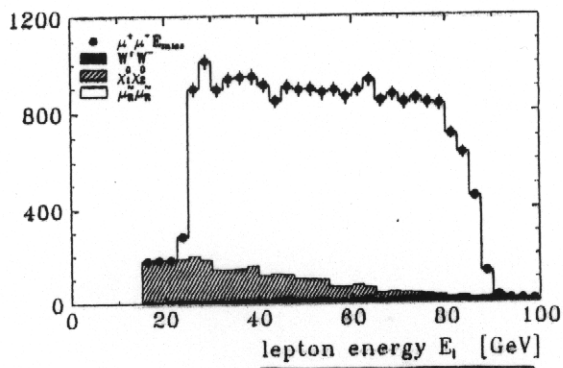
Even if the LHC "finds" them, their precise values will have to be found at the Linear Collider.

$$e^+ e^- \rightarrow \tilde{e}^+ \tilde{e}^- \rightarrow e^+ e^- \tilde{\chi}_1^0 \tilde{\chi}_1^0$$

Scalar sleptons decay isotropically in their rest frame

→ flat lepton spectrum
in lab frame

endpoints give slepton, neutralino
masses

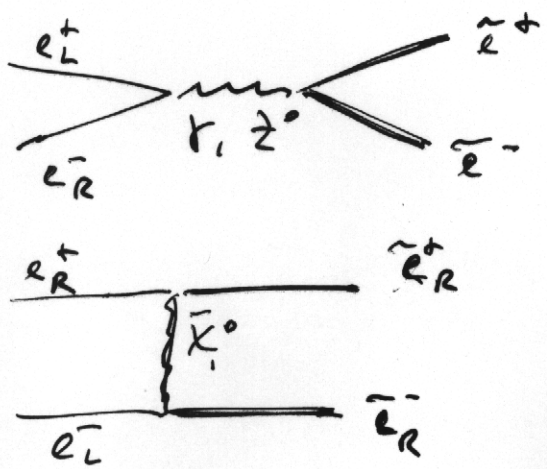


H.U. Martyn

More precise: threshold scan of production
cross section

But recall: take selection cuts,

$$\text{expect } m(\tilde{e}_L) > m(\tilde{e}_R)$$



$\sigma \sim \beta^3$
angular
momentum
barrier

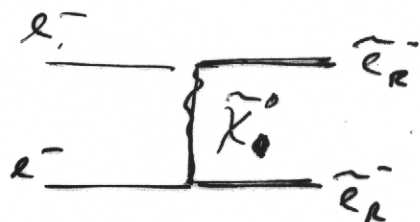
hard-to-remove
backgrounds!

But:

If we have highly polarized
 e_R^- , e_L^- beams,

study threshold q

$$e^- e^- \rightarrow \tilde{e}_R^- \tilde{e}_R^-$$



$\sigma \sim \beta$ at threshold

STEEP RISE

e_L^- switches off most backgrounds!

$$e_R^- e_L^+ \rightarrow \tilde{e}_R^- \tilde{e}_R^+ : \frac{\pi \alpha^2}{2s} \beta^3 \sin^2 \theta \left| \frac{s}{M_1^2} N_{RR}(t) - \left(1 + \frac{s_w^2}{c_w^2} \frac{s}{s - m_Z^2} \right) \right|^2$$

$$e_R^- e_L^+ \rightarrow \tilde{e}_L^- \tilde{e}_L^+ : \frac{\pi \alpha^2}{2s} \beta^3 \sin^2 \theta \left| 1 - \frac{\frac{1}{2} - s_w^2}{c_w^2} \frac{s}{s - m_Z^2} \right|^2$$

$$e_R^- e_R^+ \rightarrow \tilde{e}_R^- \tilde{e}_L^+ : \frac{2\pi \alpha^2}{s} \beta \frac{s}{M_1^2} |M_{LR}(t)|^2$$

$$e_L^- e_L^+ \rightarrow \tilde{e}_L^- \tilde{e}_R^+ : \frac{2\pi \alpha^2}{s} \beta \frac{s}{M_1^2} |M_{LR}(t)|^2$$

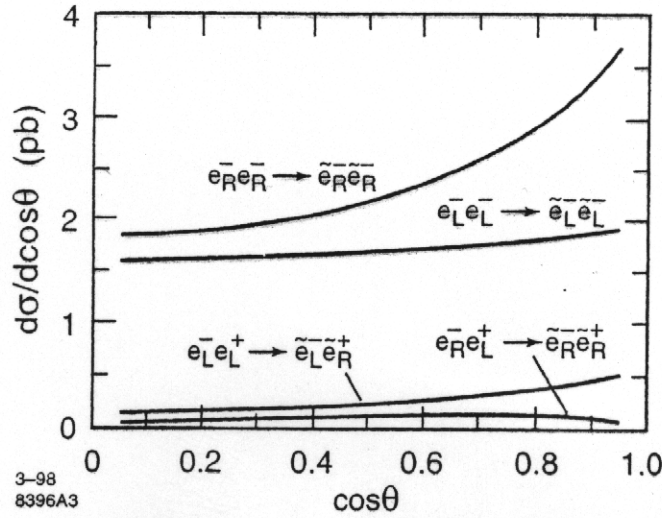
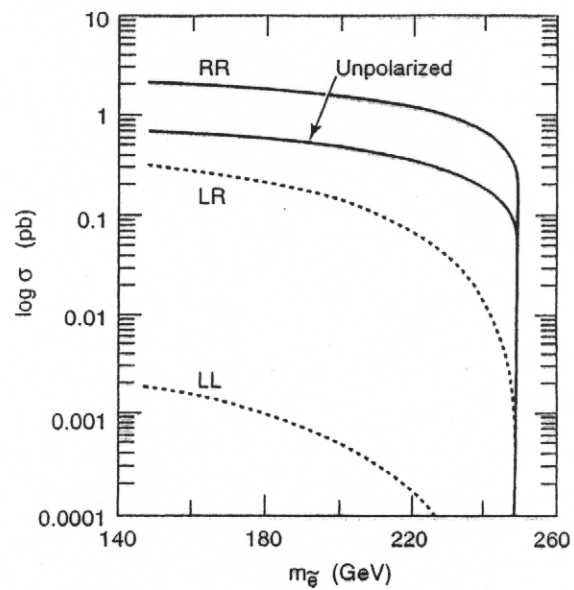
$$e_L^- e_R^+ \rightarrow \tilde{e}_R^- \tilde{e}_R^+ : \frac{\pi \alpha^2}{2s} \beta^3 \sin^2 \theta \left| 1 - \frac{\frac{1}{2} - s_w^2}{c_w^2} \frac{s}{s - m_Z^2} \right|^2$$

$$e_L^- e_R^+ \rightarrow \tilde{e}_L^- \tilde{e}_L^+ : \frac{\pi \alpha^2}{2s} \beta^3 \sin^2 \theta \left| \frac{s}{M_1^2} N_{LL}(t) - \left(1 + \frac{(\frac{1}{2} - s_w^2)^2}{c_w^2 s_w^2} \frac{s}{s - m_Z^2} \right) \right|^2$$

$$e_R^- e_R^- \rightarrow \tilde{e}_R^- \tilde{e}_R^- : \frac{2\pi \alpha^2}{s} \beta \frac{s}{M_1^2} |M_{RR}(t) + M_{RR}(u)|^2$$

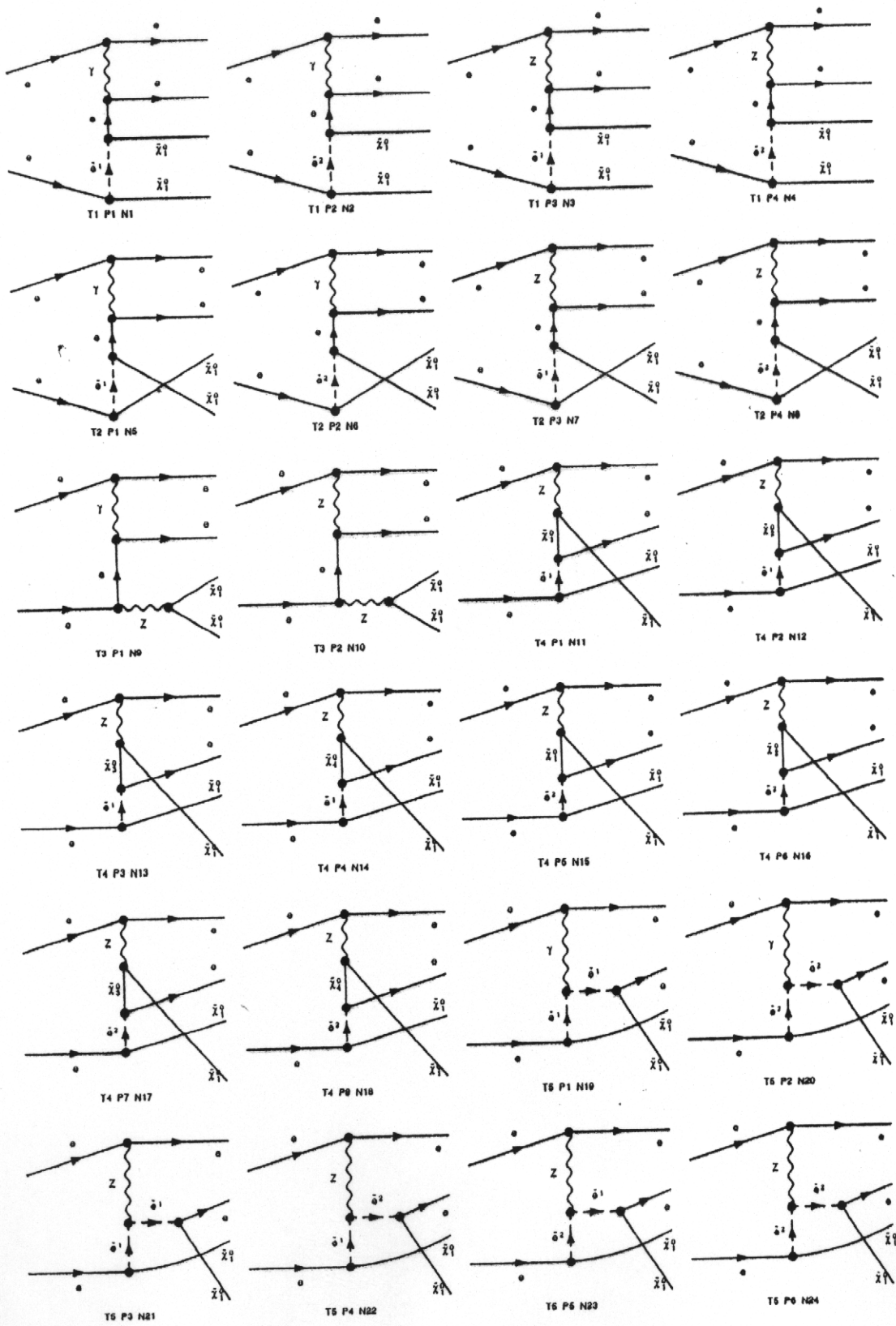
$$e_L^- e_R^- \rightarrow \tilde{e}_L^- \tilde{e}_R^- : \frac{\pi \alpha^2}{2s} \beta^3 \sin^2 \theta \left| \frac{s}{M_1^2} N_{LR}(t) \right|^2$$

$$e_L^- e_L^- \rightarrow \tilde{e}_L^- \tilde{e}_L^- : \frac{2\pi \alpha^2}{s} \beta \frac{s}{M_1^2} |M_{LL}(t) + M_{LL}(u)|^2$$



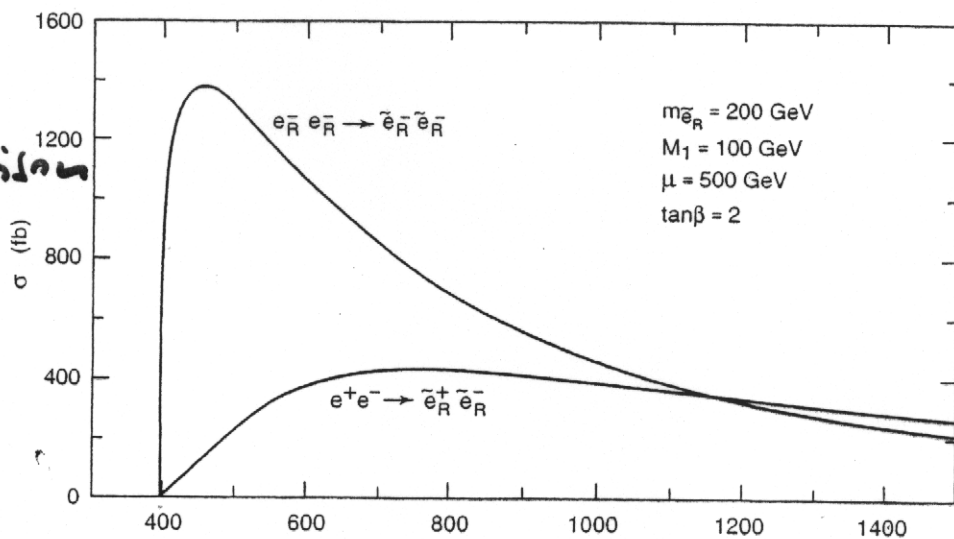
Differential cross sections for four slepton production processes, computed at a point in the Higgsino region, with $m_2/\mu = -5$ for $\tan\beta = 4$. I have taken $M_1 = 50$, $m(e_R) = 150$, $m(e_L) = 200$, $\sqrt{s} = 500$ GeV.

$$\theta \quad \theta \rightarrow \theta \quad \theta \quad \tilde{\chi}_1^0 \quad \tilde{\chi}_1^0$$

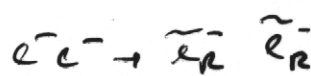


before \tilde{e}^- width, branching ratios, and 'cos's

rough
comparison



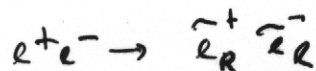
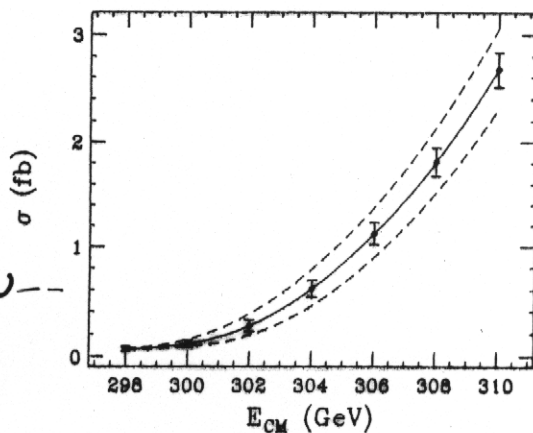
Feng & Peskin comparison



$$P_{e^-} = 0.8$$

$$\Delta m_{\tilde{e}_R} = \pm 100 \text{ MeV}$$

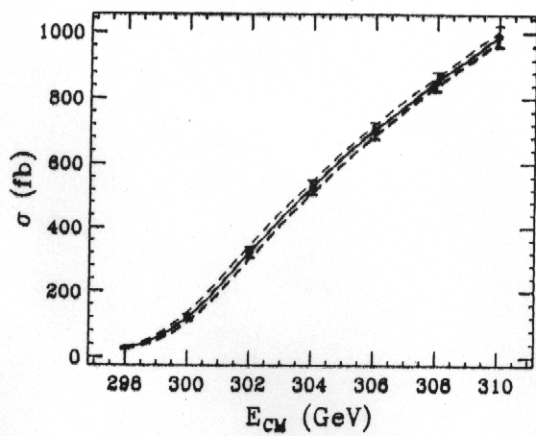
1 fb⁻¹ per point



$$P_{e^+} = 0, P_{e^-} = 0.8$$

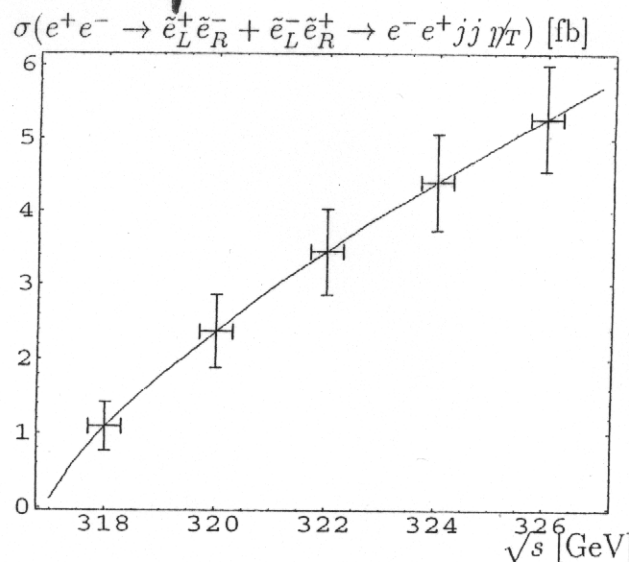
$$\Delta m_{\tilde{e}_R} = \pm 400 \text{ MeV}$$

100 fb⁻¹ per point



threshold scan for e^+e^-

note the small slope.

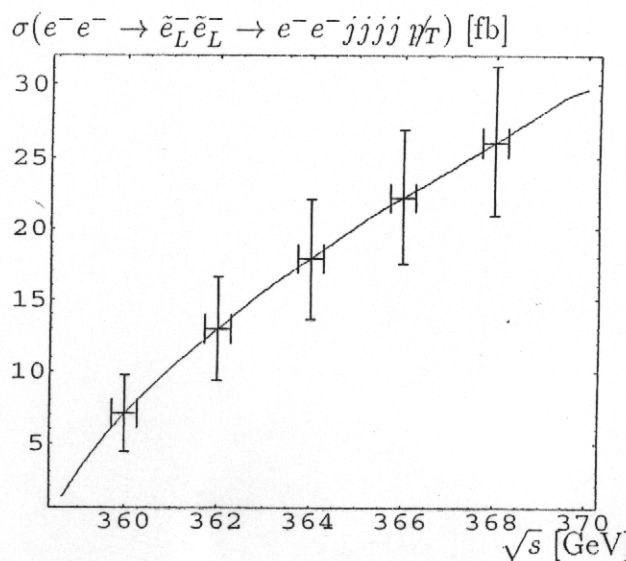


low e^+
pol.,

$m(\tilde{e}_L \neq \tilde{e}_R)$
make for
poor
threshold
quality

Threshold behaviour of the processes $e^+e^- \rightarrow \tilde{e}_L^+\tilde{e}_R^- + \tilde{e}_L^-\tilde{e}_R^+ \rightarrow e^-e^+jj p_T$ for $P_{e^-} = 0.8$ and $P_{e^+} = 0.6$, $M_2 = 152$ GeV, $\mu = 316$ GeV and $\tan\beta = 3$. ISR corrections and beamstrahlung are included. The error bars show the statistical error for $\mathcal{L} = 10 \text{ fb}^{-1}$.

... and for e^-e^-



clean
signal,
well-defined
mass
resolution!

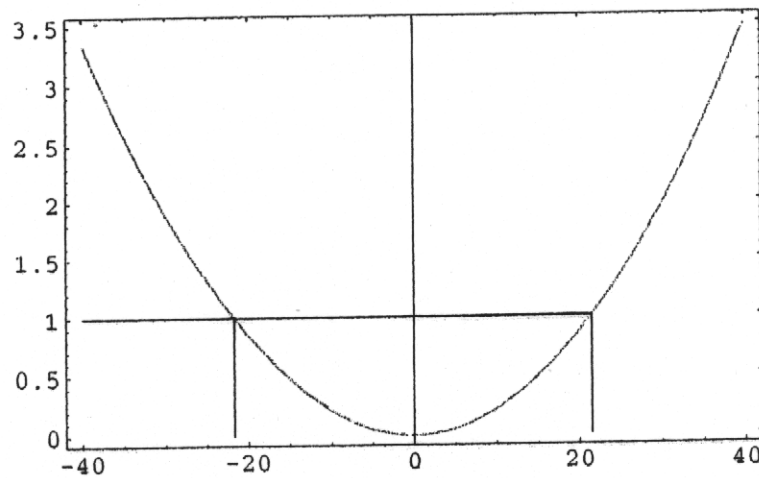
Threshold behaviour of the process in $e^-e^- \rightarrow \tilde{e}_L^-\tilde{e}_L^- \rightarrow e^-e^-jjjj p_T$ for $P_{e_1} = -0.8$ and $P_{e_2} = -0.8$. ISR corrections and beamstrahlung are included. The error bars show the statistical error for $\mathcal{L} = 1 \text{ fb}^{-1}$.

Blochinger and Mayer, in preparation

- calculated the total cross section of

$$e^- e^- \rightarrow \tilde{e}_{L/R}^- \tilde{e}_{L/R}^- \rightarrow e^- e^- \tilde{\chi}_1^0 \tilde{\chi}_1^0$$

- Include ISR and beamstrahlung (use **Pandora**)
- Perform χ^2 fit and find:

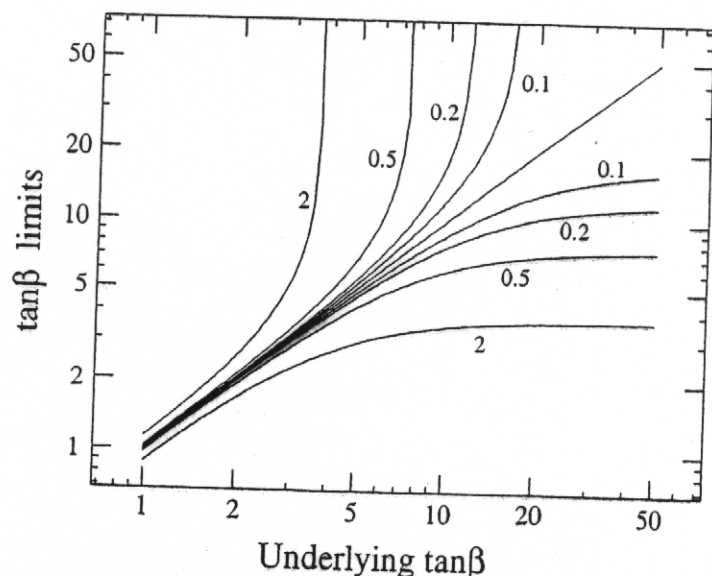


$$\Delta m_{\tilde{e}_R} \approx 22 \text{ MeV} \text{ with } 1 \text{ fb}^{-1}$$

- For the left selectron an error of 400-500 MeV is feasible (preliminary)

Why do we want such precise information
on selection etc. masses?

ACCESS TO $\tan \beta$



Contours giving the upper and lower limits on $\tan \beta$ for a given underlying $\tan \beta$ and experimental uncertainty in mass difference $\Delta m \equiv m_{\tilde{\nu}_L} - m_{\tilde{\nu}_e}$ as indicated (in GeV), for fixed $m_{\tilde{\nu}_e} = 200$ GeV.

Recall that, at tree level

$$m_{\tilde{\nu}_L}^2 - m_{\tilde{\nu}_e}^2 = -M_W^2 \cos 2\beta$$

↑ ↑ ↗
we measure this we know this

2nd Generation:

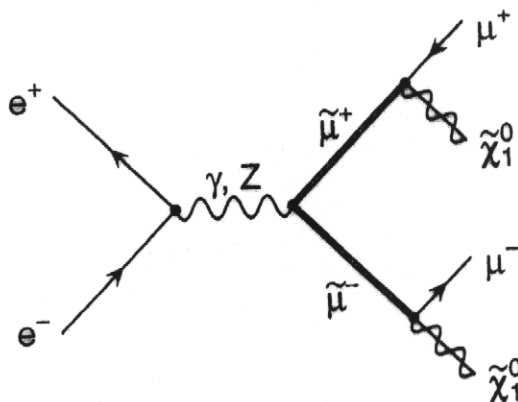
3.

collisions

- s-channel γ, Z exchange
- P-wave \Rightarrow Cross-section $\sim \beta^3$ at threshold
- Restrict to $\tilde{\mu}_R^+ \tilde{\mu}_R^-$ for simplicity
- Dominant decay $\tilde{\mu}_R^- \rightarrow \mu^- \tilde{\chi}_1^0$

choose this
final state

ISIDORI



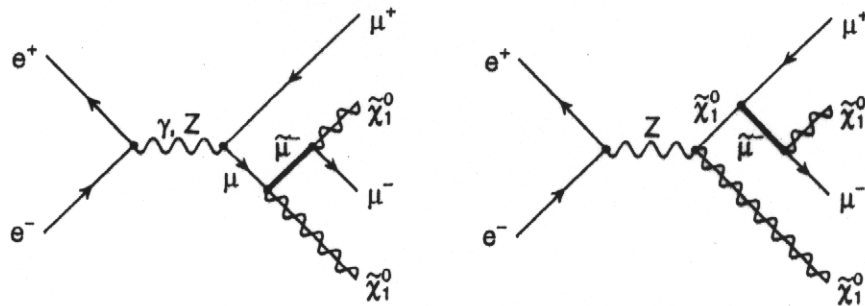
for easy
muon
detection

Double resonant graph is gauge dependent.

One can get any answer one likes!

Note:

⇒ Must include singly resonant graphs in signal
to give gauge invariant result



- Include finite width by introducing the complex mass



$$m_\mu^2 \rightarrow M_\mu^2 = m_\mu^2 - i m_\mu \Gamma_\mu$$

- Cannot use double pole approximation at threshold
- Many more singly and non-resonant graphs which are now considered as backgrounds
- Signal and background amplitudes calculated using **Feynarts**
- Adaptive weight optimised Monte Carlo integration over phase space
- ISR included using structure function method
- Beamstrahlung included using **CIRCE**

ATTENTION: Unlike in the Selection case,
We now have large **BACKGROUNDS**

Backgrounds: $e^+e^- \rightarrow \mu^+\mu^- + E$

[backgrounds easy to remove]

[Blair, Martyn]

- 1. $e^+e^- \rightarrow W^+W^-, W \rightarrow \mu\nu$
- 2. $e^+e^- \rightarrow (\gamma/Z)(\gamma/Z), \gamma/Z \rightarrow \mu^+\mu^-, \gamma/Z \rightarrow \nu\bar{\nu}$

Remove 1: W decay leptons lie approx. in an azimuthal plane.

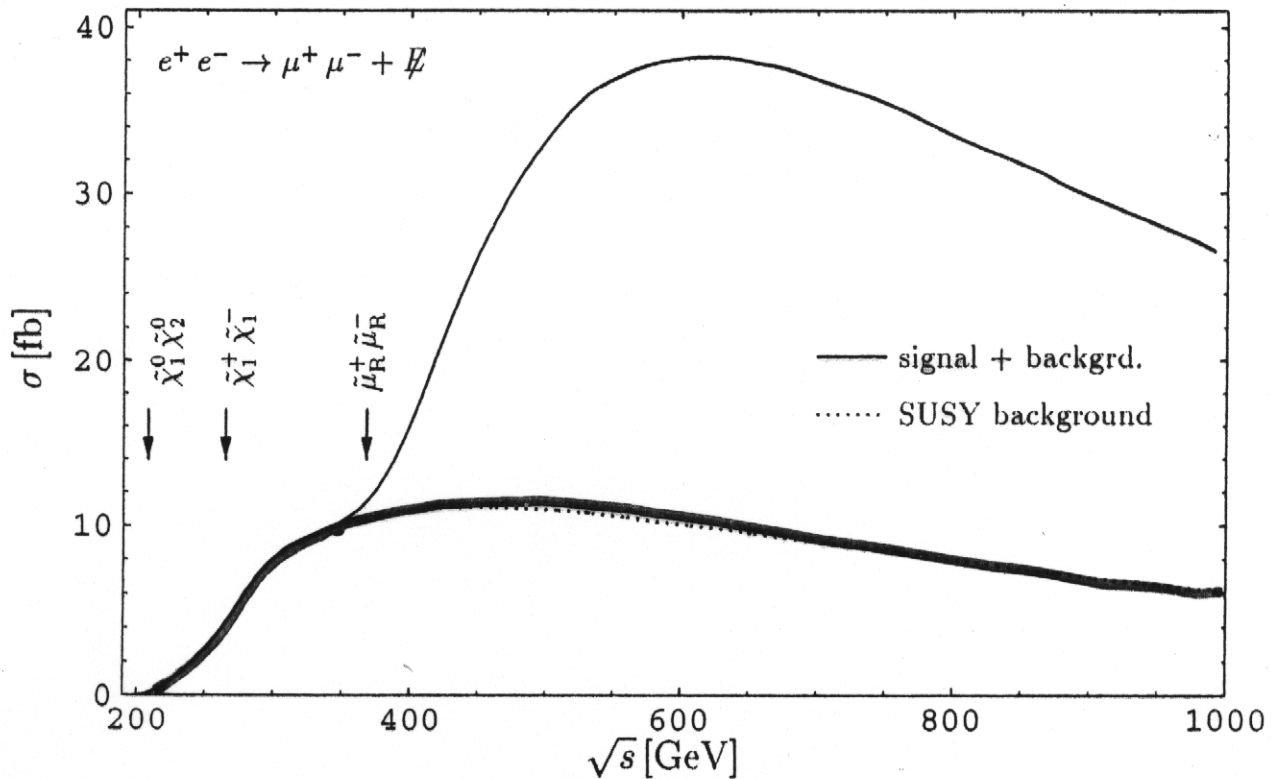
Remove 2: cut lepton pairs which are:

- collinear
- have invariant mass near the Z mass.

Cuts and detector acceptance \rightarrow signal efficiency of 50%

Main SUSY backgrounds:

- $e^+e^- \rightarrow \tilde{\chi}_k^0\tilde{\chi}_1^0, \tilde{\chi}_k^0 \rightarrow \mu^+\mu^-\tilde{\chi}_1^0$
- $e^+e^- \rightarrow \tilde{\chi}_2^0\tilde{\chi}_2^0, \tilde{\chi}_2^0 \rightarrow \mu^+\mu^-\tilde{\chi}_1^0, \tilde{\chi}_2^0 \rightarrow \nu\bar{\nu}\tilde{\chi}_1^0$
- $e^+e^- \rightarrow \tilde{\chi}_1^+\tilde{\chi}_1^-, \tilde{\chi}_1^\pm \rightarrow \tilde{\mu}^\pm\nu_{\tilde{\mu}}\tilde{\chi}_1^0$
- $e^+e^- \rightarrow ZZ, Z \rightarrow \mu^+\mu^-, Z \rightarrow \tilde{\chi}_1^0\tilde{\chi}_1^0$
- $e^+e^- \rightarrow Zh_0/H_0, Z \rightarrow \mu^+\mu^-, h_0/H_0 \rightarrow \tilde{\chi}_1^0\tilde{\chi}_1^0$



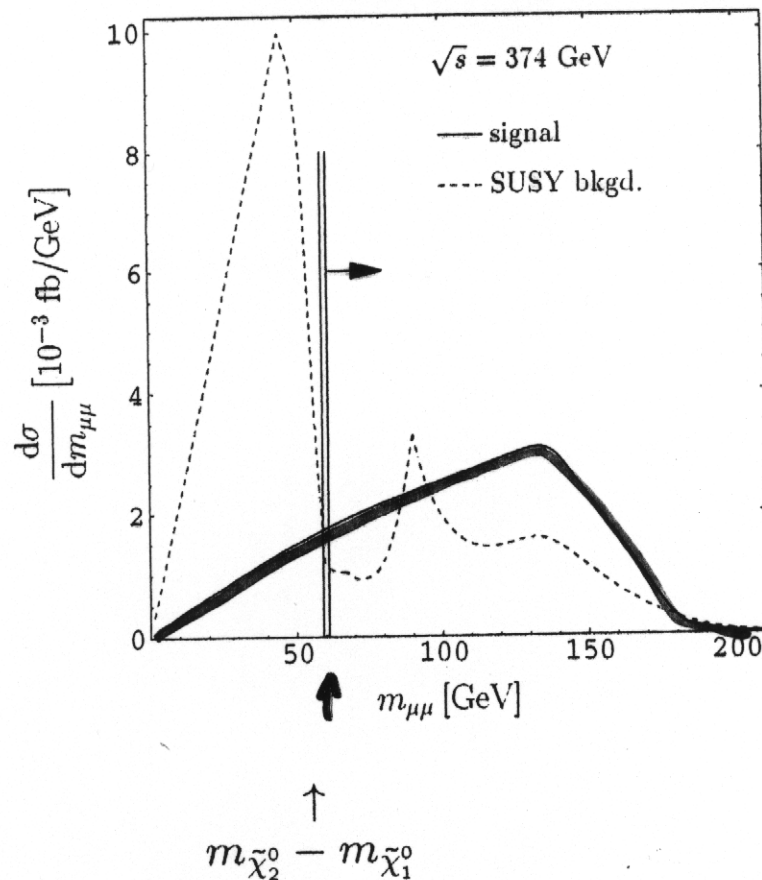
Removal of SUSY backgrounds

1. Cascade decays \Rightarrow extra missing energy



Cuts < 30 GeV/s

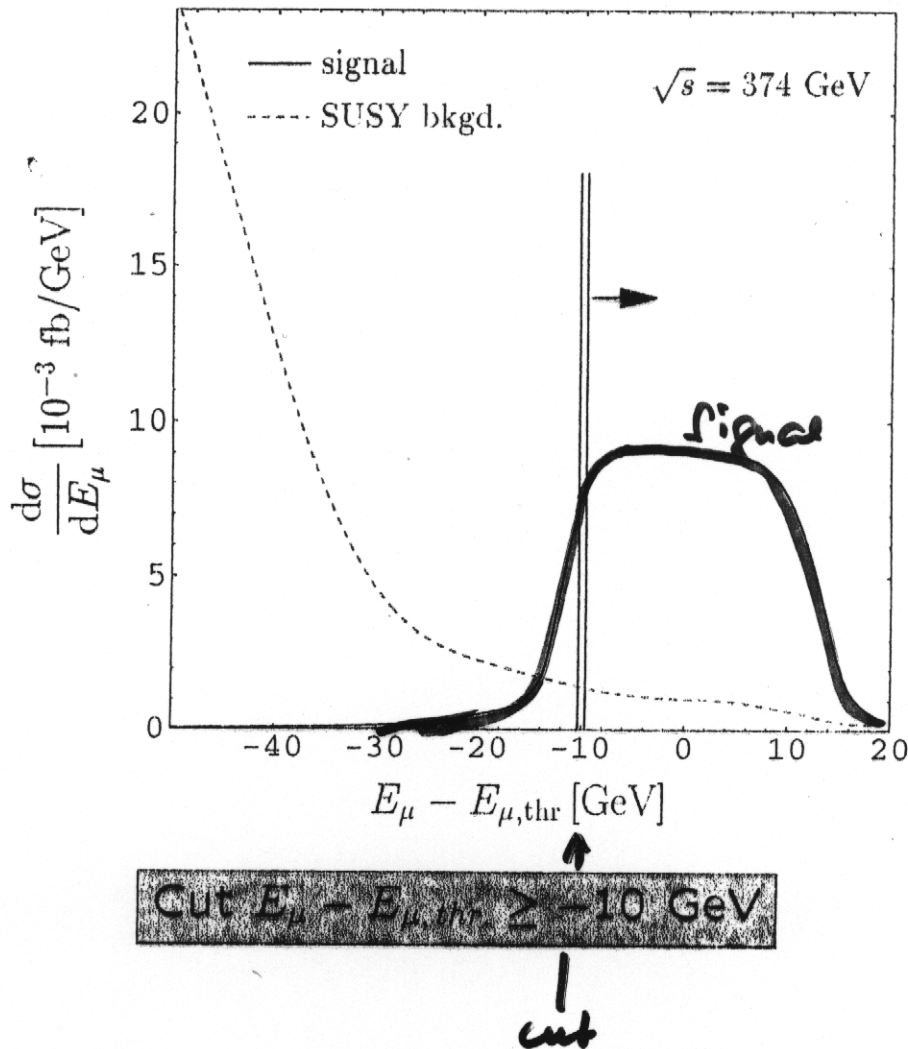
Then make cut on muon pair invariant mass:



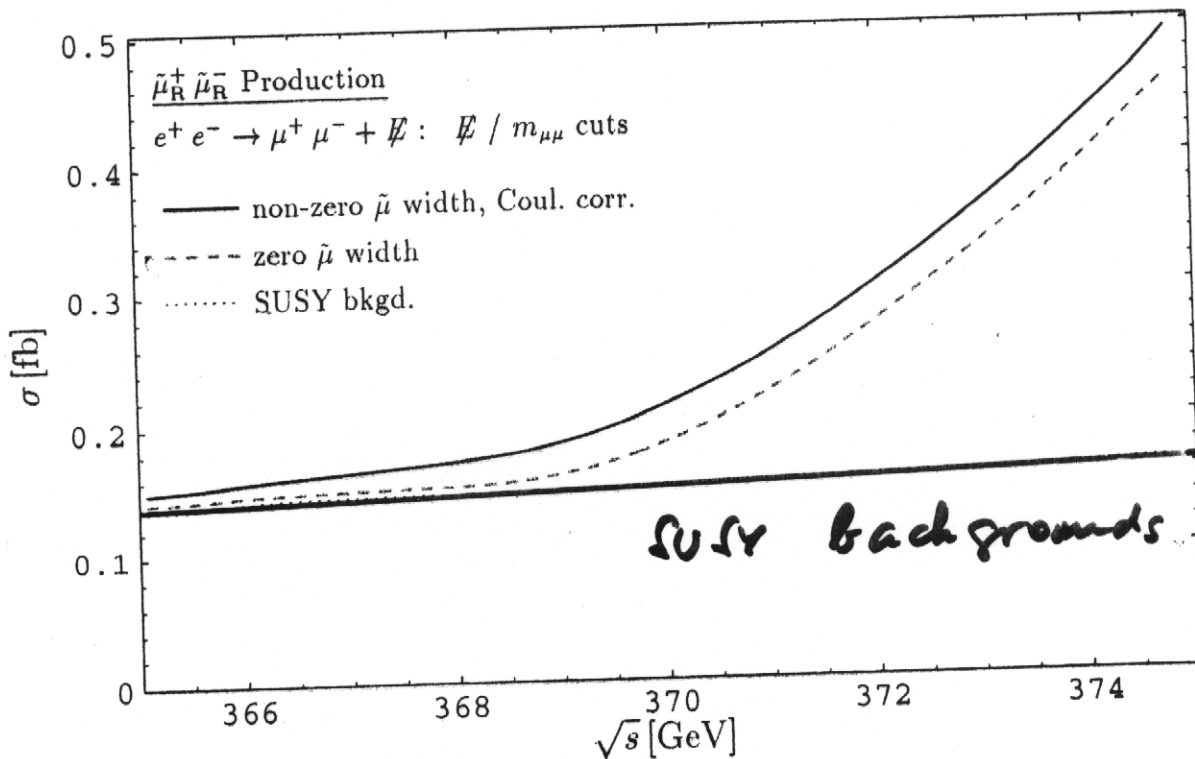
OR -

Alternatively:

2. Signal: Muon energies near threshold energy
Background: Much lower E_μ



Results



Remaining backgrounds smooth over threshold region
 ↓
 Remove in a model independent way by extrapolating
 from below

Conclusions on \tilde{e} 's, $\tilde{\mu}$'s



- e^-e^- option much better than e^+e^- for measuring selectron mass
- Negligible backgrounds
- Very accurate mass measurement with little luminosity



- More theoretically challenging
- Must beware of gauge dependence
- Cuts can be devised to remove backgrounds
- Accurate mass measurement looks promising

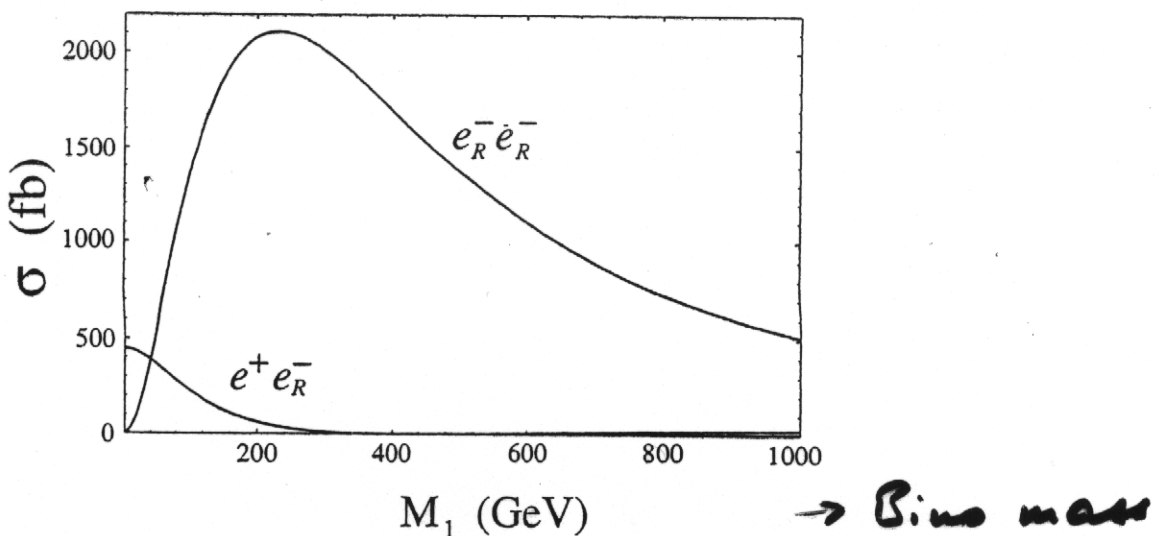
Must include radiative corrections for
per mille accuracy



Work on this underway

GAUGINO, NEUTRALINO MASSES

Supersymmetry at Linear Colliders: The Importance of Being e^-e^- 2327



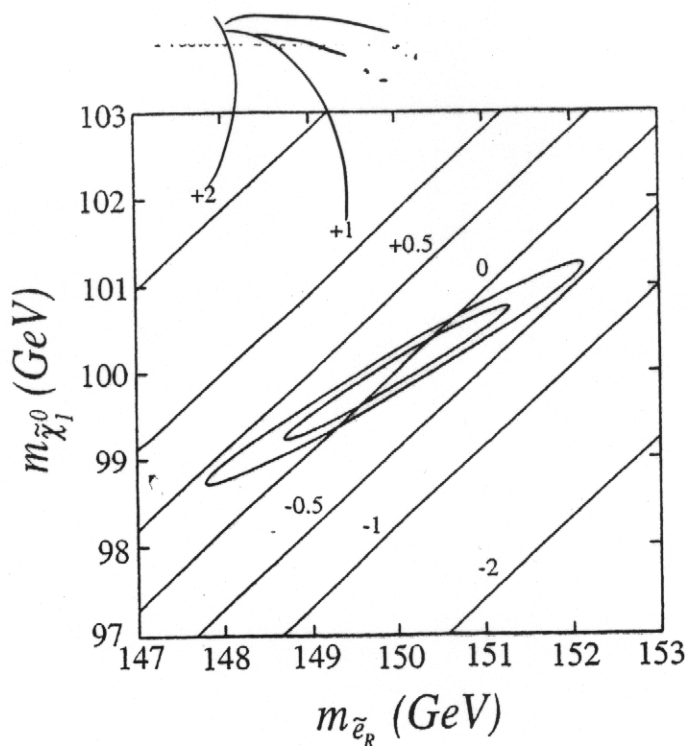
Cross sections for $\sigma(e_R^- e_R^- \rightarrow \tilde{e}_R^- \tilde{e}_R^-)$ and $\sigma(e^+ e_R^- \rightarrow \tilde{e}_R^+ \tilde{e}_R^-)$ as functions of the Bino mass M_1 for $m_{\tilde{e}_R} = 200$ GeV and $\sqrt{s} = 500$ GeV. The t -channel mass insertion for the e^-e^- case leads to large cross sections, even for $M_1 \sim \mathcal{O}(1)$ TeV.

for $\sqrt{s} = 500$ GeV

$\sigma(\tilde{e}_R^- \tilde{e}_R^-)$ - which we measure
precisely -

determines the bino mass
precisely once we know $m(\tilde{e}_R^-)$.

difference in % of σ_R from the central value parameters



Uncertainty ellipses

determined by

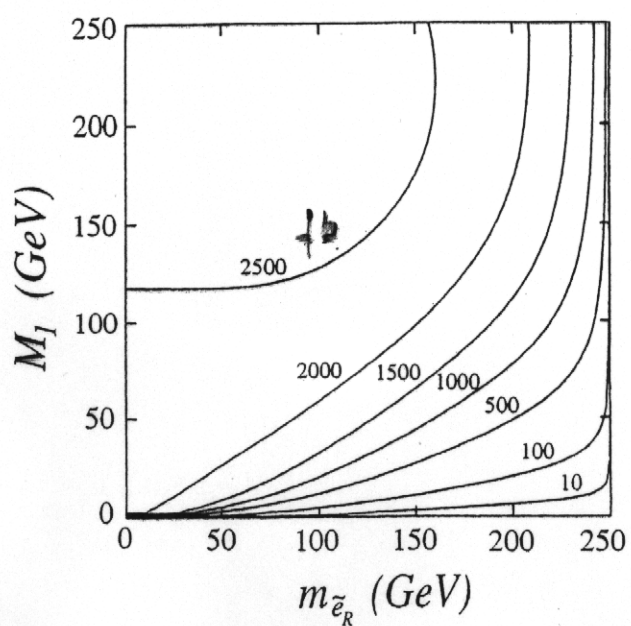
final-state electron
energy endpoints

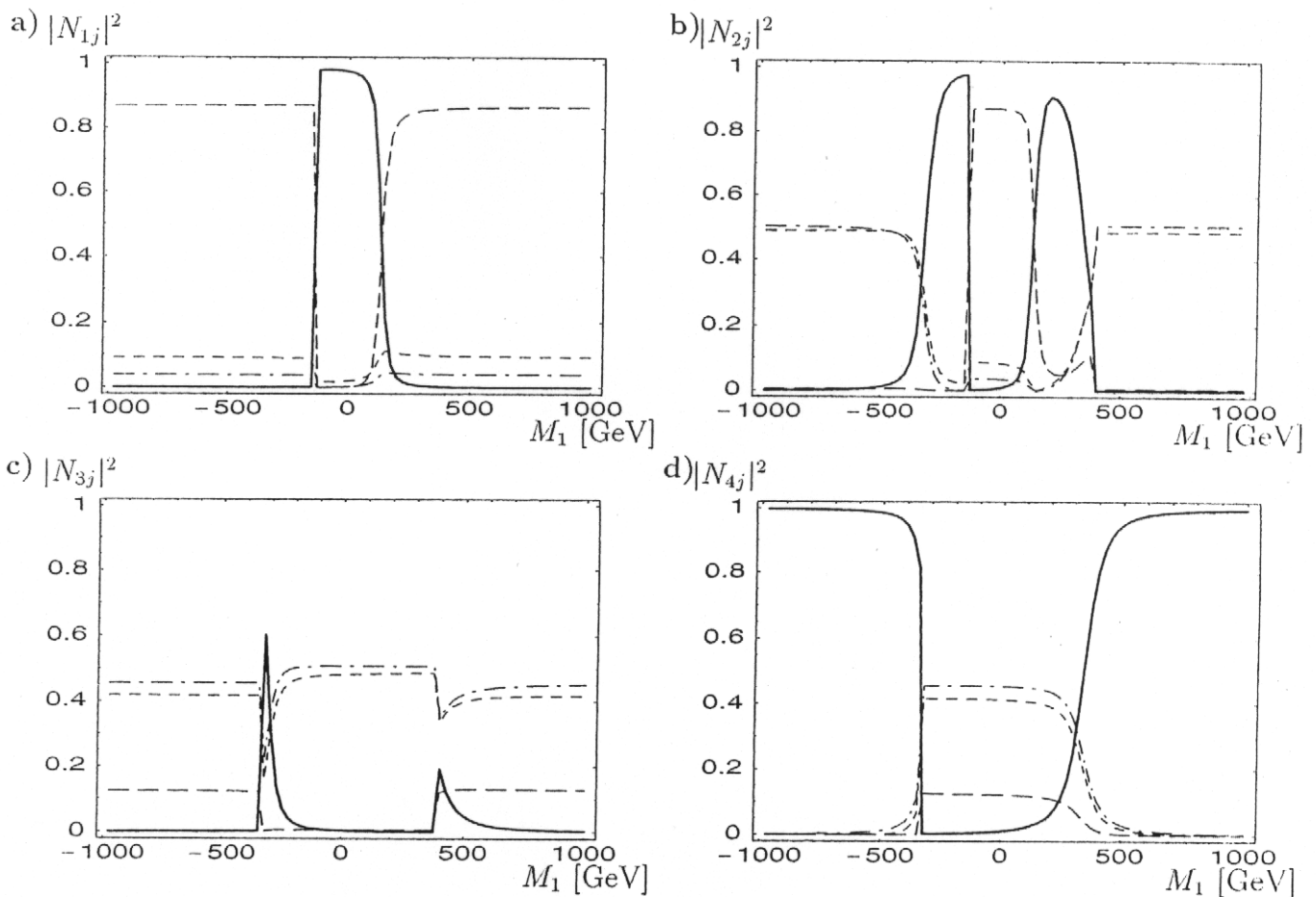
at $\sqrt{s} = 0.5 \text{ TeV}$

assuming $m_{tilde{e}_R} = 150 \text{ GeV}$

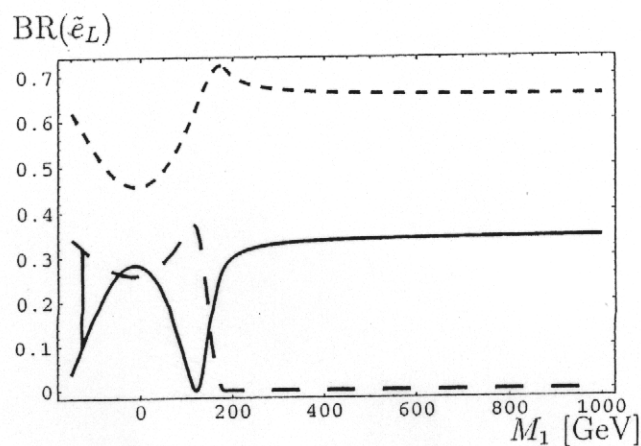
$m_{tilde{χ}_1^0} = 100 \text{ GeV}$

Measure $\tau(\tilde{e}_R \tilde{e}_R)$, find M_1 (or $m_{tilde{e}_R}$)
if not previously known

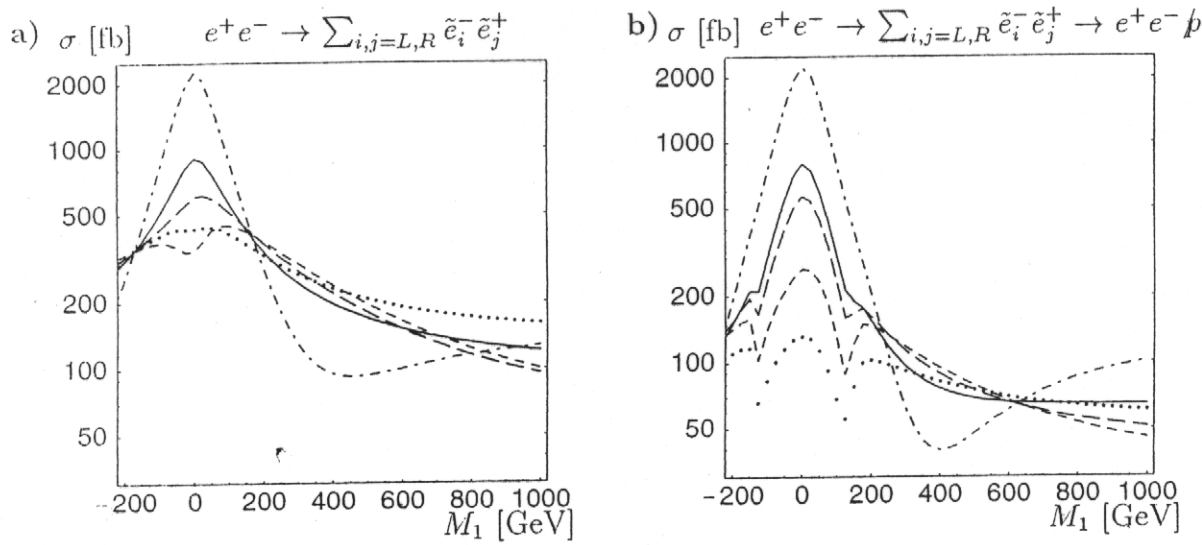




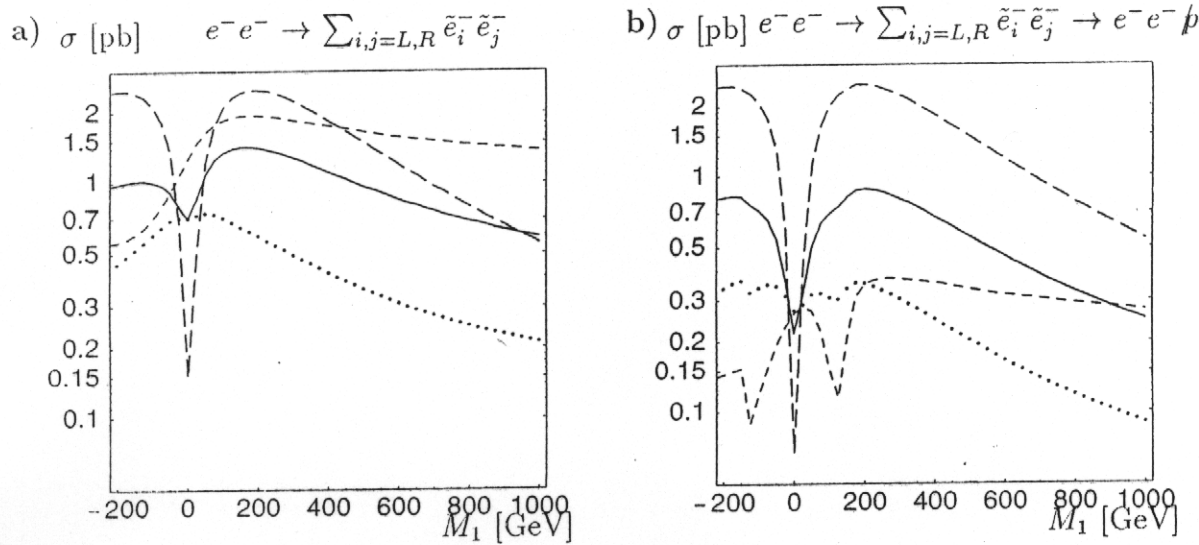
a) $|N_{1j}|^2$, b) $|N_{2j}|^2$, c) $|N_{3j}|^2$, and d) $|N_{4j}|^2$ as a function of M_1 for $M_2 = 152$ GeV, $\mu = 316$ GeV and $\tan \beta = 3$. The graphs correspond to the following components: full line \tilde{B} , long dashed line \tilde{W}_3 , dashed line \tilde{H}_d^0 and long short dashed line \tilde{H}_u^0 .



Branching ratios of \tilde{e}_L as a function of M_1 for $m_{\tilde{e}_L} = 179.3$ GeV, $M_2 = 152$ GeV, $\mu = 316$ GeV and $\tan \beta = 3$. The graphs correspond to: full line $BR(\tilde{e}_L \rightarrow \tilde{\chi}_1^0 e^\pm)$, long dashed line $BR(\tilde{e}_L \rightarrow \tilde{\chi}_2^0 e^\pm)$ and dashed line $BR(\tilde{e}_L \rightarrow \tilde{\chi}_1^\pm \nu_e)$.



Cross sections for the processes $\sigma(e^+e^- \rightarrow \sum_{i,j=L,R} \tilde{\epsilon}_i^- \tilde{\epsilon}_j^+)$ (a) and $\sigma(e^+e^- \rightarrow \sum_{i,j=L,R} \tilde{\epsilon}_i^- \tilde{\epsilon}_j^+ \rightarrow e^+e^- p_T)$ (b) as a function of M_1 for various polarizations. The effects of ISR- and beamstrahlung corrections are included. The graphs correspond to the following set of polarizations: full line $P_{e^-}=0, P_{e^+}=0$, dashed line $P_{e^-}=-0.8, P_{e^+}=-0.6$, dashed-dotted line $P_{e^-}=0.8, P_{e^+}=-0.6$, dotted line $P_{e^-}=-0.8, P_{e^+}=0.6$, and long dashed line $P_{e^-}=0.8, P_{e^+}=0.6$.



Cross sections for the processes $\sigma(e^-e^- \rightarrow \sum_{i,j=L,R} \tilde{\epsilon}_i^- \tilde{\epsilon}_j^-)$ (a) and $\sigma(e^-e^- \rightarrow \sum_{i,j=L,R} \tilde{\epsilon}_i^- \tilde{\epsilon}_j^- \rightarrow e^-e^- p_T)$ (b) as a function of M_1 for various polarizations. The effects of ISR- and beamstrahlung corrections are included. The graphs correspond to the following set of polarizations: full line $P_{e_1}=0, P_{e_2}=0$, dashed line $P_{e_1}=-0.8, P_{e_2}=-0.8$, dotted line $P_{e_1}=-0.8, P_{e_2}=0.8$, and long dashed line $P_{e_1}=0.8, P_{e_2}=0.8$.

NEUTRALINO

CP-VIOLATING PHASES?

1st-order effect possible in $e_L^+ e_L^- \rightarrow \tilde{e}_L^+ \tilde{e}_L^-$

$e^+ e^- : \tilde{e}_L^\pm \tilde{e}_R^\mp$ requires 2nd order in mixing

$e^- e^- : \tilde{e}_R^\pm \tilde{e}_R^\mp \quad \langle BB \rangle$ only: no interference

$e_L^+ e_L^- \quad \langle BB \rangle, \langle WW \rangle :$

m, m_2^* interference

Work by Scott Thomas

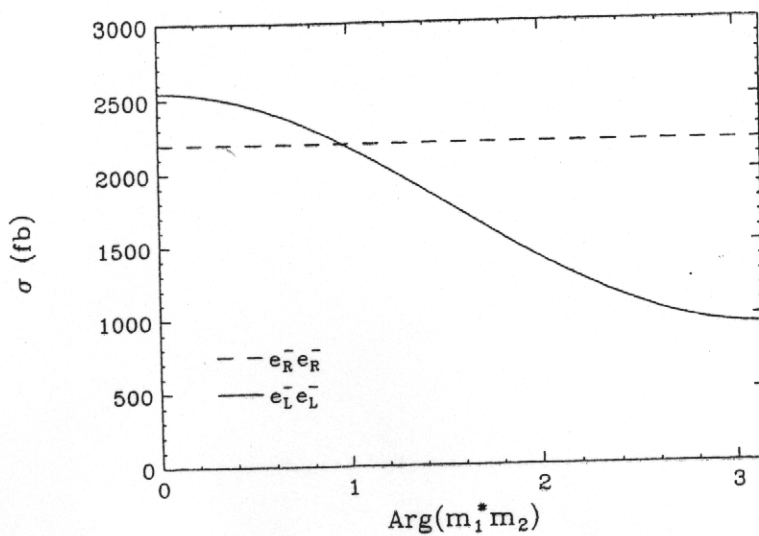
$$\mathcal{L} = -\frac{1}{2}\lambda M \lambda + h.c.$$

$$M = \begin{pmatrix} m_1 & 0 & -(g'/\sqrt{2})H_d^{0*} & (g'/\sqrt{2})H_u^{0*} \\ 0 & m_2 & (g/\sqrt{2})H_d^{0*} & -(g/\sqrt{2})H_u^{0*} \\ -(g'/\sqrt{2})H_d^{0*} & (g/\sqrt{2})H_d^{0*} & 0 & -\mu \\ (g'/\sqrt{2})H_u^{0*} & -(g/\sqrt{2})H_u^{0*} & -\mu & 0 \end{pmatrix}$$

In $e_L^- e_L^- \rightarrow \tilde{e}_L^- \tilde{e}_L^-$, the interference term is important:

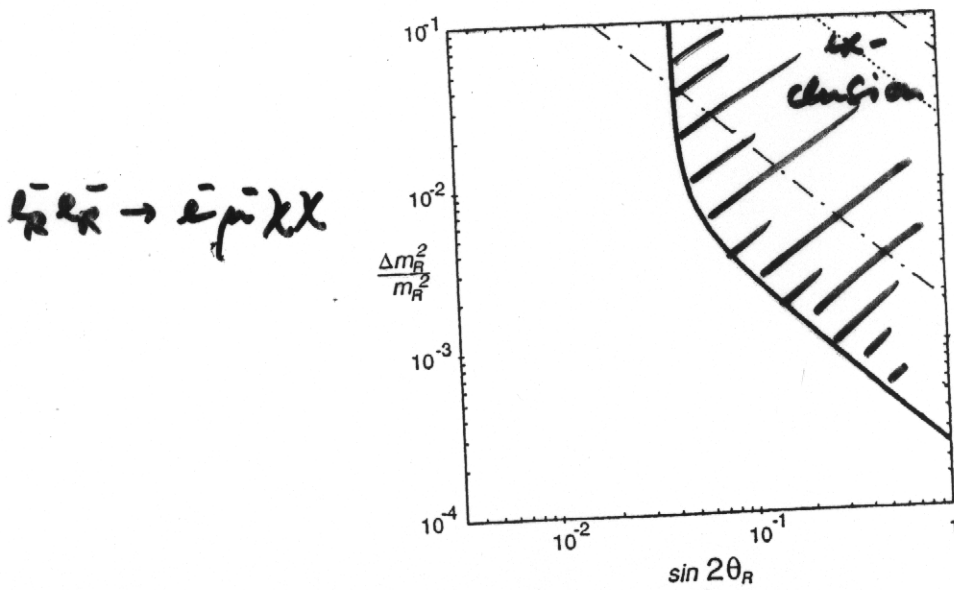
$$|M_{LL}(t)|^2 = \frac{1}{16 \sin^4 \Theta_W} \left(\frac{|m_1|^2 \tan^4 \Theta_W}{(|m_1|^2 - t)^2} + \frac{2|m_1||m_2| \tan^2 \Theta_W \cos(\arg(m_1^* m_2))}{(|m_1|^2 - t)(|m_2|^2 - t)} + \frac{|m_2|^2}{(|m_2|^2 - t)^2} \right)$$

leading to a highly observable effect:



SLEPTON FLAVOR MIXING

Flavor violation is permitted in SUSY
 (as at neutral gaugino vertices)



Reach in
 view of
 $B(\mu \rightarrow e\gamma)$

assumed parameters: The discovery reach (solid) for lepton flavor violation through the signal $e_R^- e_R^- \rightarrow e^- \mu^- \chi \chi$ for 200 GeV slepton masses, $m_\chi = 100$ GeV, $\sqrt{s} = 500$ GeV, and an integrated luminosity $L = 20 \text{ fb}^{-1}$. Regions of the plane to the upper-right are excluded by the current bound $B(\mu \rightarrow e\gamma) < 4.9 \times 10^{-11}$ for $\ell = 0$ (dotted), 2 (dashed), and 50 (dot-dashed), where we have assumed $m_{\tilde{t}_L} = 350$ GeV.

In principle, there is room for 7 new CKM matrices
 — one for each { fermion } species
 { sfermion }

$$f = u_L, u_R, d_L, d_R, e_L, e_R, \nu$$